J. Membrane Biol. 49, 1–20 (1979)

Volume Flows across Gallbladder Epithelium Induced by Small Hydrostatic and Osmotic Gradients

Carel H. van Os, Günther Wiedner, and Ernest M. Wright*

Department of Physiology, University of Nijmegen, Nijmegen, The Netherlands and Max Planck Institut of Biophysics, Frankfurt a.M., G.F.R.

Received 15 December 1978

Summary. The hydraulic conductivity of rabbit gallbladder epithelium has been studied using a continuous volumetric method based on capacitance measurements. The time resolution for measuring osmotic flows is in the range of seconds. Volume flows have been induced by osmotic gradients between 0 and 100 mosmol. In this range the flow-force relation is linear and the P_f value is 9.3×10^{-3} cm/sec. After correction for solute polarization effects, the P_f value amounts to 0.05 cm/sec. The observed flow is constant between 5 sec up to 20 min after a sudden increase in the osmolarity of the mucosal solution. The wet weight of the gallbladder tissue decreases by 22% and increases by 30% during osmotic flows from serosa to mucosa and from mucosa to serosa, respectively. Volume flows induced by hydrostatic pressure gradients on the mucosal surface are linearly related to the driving forces between 0 and 40 mbar. The P_f value is 0.15 cm/sec. The volume flows are constant between 2 sec and 15 min after pressure application. The flow-force relation for pressure gradients on the serosal surface is markedly nonlinear for gradients greater than 5 mbar. Below 5 mbar the P_f value is 4.5 cm/sec. From electrical measurements, e.g., resistance and streaming potentials, and from flux studies with inulin and polyethylene glycol 4000, it is concluded that hydrostatic and osmotic gradients are not comparable when they are applied to gallbladder epithelium. They induce volume flows across different pathways, e.g., osmosis predominantly across the cellular route and pressure filtration predominantly across paracellular routes.

Isotonic reabsorbing epithelia are expected to have a high hydraulic conductivity, L_p or P_f, to account for rapid water movements coupled to active solute transport. Unfortunately attempts to estimate the magnitude of the L_p, of, for example, gallbladder epithelium are hindered by several factors. The thick supporting connective tissue layer has been shown to be the site of solute polarization effects during osmosis (Wright, Smulders & Tormey, 1972; Lerche, 1976). Hence, applied gradients of sucrose are effectively reduced by build-up of oppositely directed salt gradients in unstirred layers, thereby reducing the applied osmotic gra-

* *Permanent address:* Department of Physiology, University of California, Medical Center, Los Angeles, U.S.A.

0022-2631/79/0049-0001 $04.00

dient by a factor of five (Wright *et al.*, 1972). In addition, these volume flows were measured gravimetrically with time intervals of 5 min. Since in everted sacs osmotic flow rates decreased to one-fifth of the initial rate within 5 min after application of an osmotic gradient to the mucosal surface, time resolution of 5 min is largely inadequate (Wright *et al.*, 1972). Recently a method has been developed to detect volume flows continuously with sensitivities in the nanoliter range (Wiedner, 1976). We have used this method to monitor volume flows induced by small gradients across the gallbladder.

A large discrepancy between L_p values obtained from hydrostatic and osmotic pressure gradients have been observed in all epithelia studied so far (House, 1974). Apparently epithelial membranes are in a different state of reference, depending on what driving force is acting on them. To find out why hydrostatic pressure is more effective than osmotic forces we have studied both driving forces in rabbit gallbladder, using the continuous volumetric method. In addition, we have studied the permeability of various nonelectrolytes before, during, and after application of hydrostatic and osmotic pressure gradients to see whether these forces have effects on nonelectrolyte fluxes and whether solvent drag effects can be observed. Occurrence of solvent drag effects on nonelectrolyte fluxes may provide an answer to the question whether the route of water is predominantly cellular or paracellular.

Materials and Methods

Gallbladders are obtained from albino rabbits of both sexes. After dissection and removal of bile, the bladders are cut open and left in gassed solutions (100% O_2) at room temperature until they are mounted between two Lucite rings. Ringer's solution of the following composition has been used (in mM): NaCl, 145; KCl, 5; $CaCl_2$, 0.25; $MgCl_2$, 1.0; NaH_2PO_4, 0.375; Na_2HPO_4, 2.125; pH, 7.4. Sucrose is used to increase the osmolarity of Ringer's solutions. The osmolarity of solutions are measured with an Advanced Osmometer, type 3A.

During osmosis the wet wt of the gallbladder wall changes. These changes have been measured as follows: Gallbladder sheets are clamped between two Lucite rings. Then, one of the surfaces is exposed to Ringer's solution while the other side is in contact with a Ringer's solution containing additional sucrose. Tissue wet wt of 0.78 cm^2 tissue can be determined by weighing the rings plus gallbladder and subtracting the weight of the rings.

Volumetric Flow Measurements

Flat sheets of gallbladder tissue are stretched and clamped between two Lucite rings. Soft silicone rubber rings on either side of the tissue are used to circumvent edge damage.

The Lucite rings function as a frame holding the tissue. This frame is mounted between two Lucite half chambers (Fig. 1). The surface area of the bladder exposed to the bathing solutions can be varied between 0.03 and 0.78 cm^2 using different frames. No support has been used. Volume flows across the gallbladder are detected by making use of capacitance measurements described previously (Wiedner, 1976). When a probe is placed near a conducting surface, a capacitance exists between this surface and the probe head. A change in capacitance is a measure of a change in distance between the probe and the liquid surface. A decrease in volume of one of the two half chambers results in an increase in the distance, hence a decrease in capacitance. The experimental arrangement is sketched in Fig. 1. Capacitance is measured using the commercially available DIMEQ TE 200 transducer equipment (Wayne Kerr, Bognor Regis, England). The volumes of both half chambers are monitored continuously and plotted on a three-channel pen recorder (Rikadenki B35), using one channel for each probe and the third channel for the display of the difference between both probe signals. Measuring volume changes on both sides is imperative in any experimental arrangement of sufficient accuracy. In our experiments volume changes can be observed which are not directly related to flow across the gallbladder; e.g., evaporation or volume uptake by the Lucite chamber. In order to be able to increase the pressure

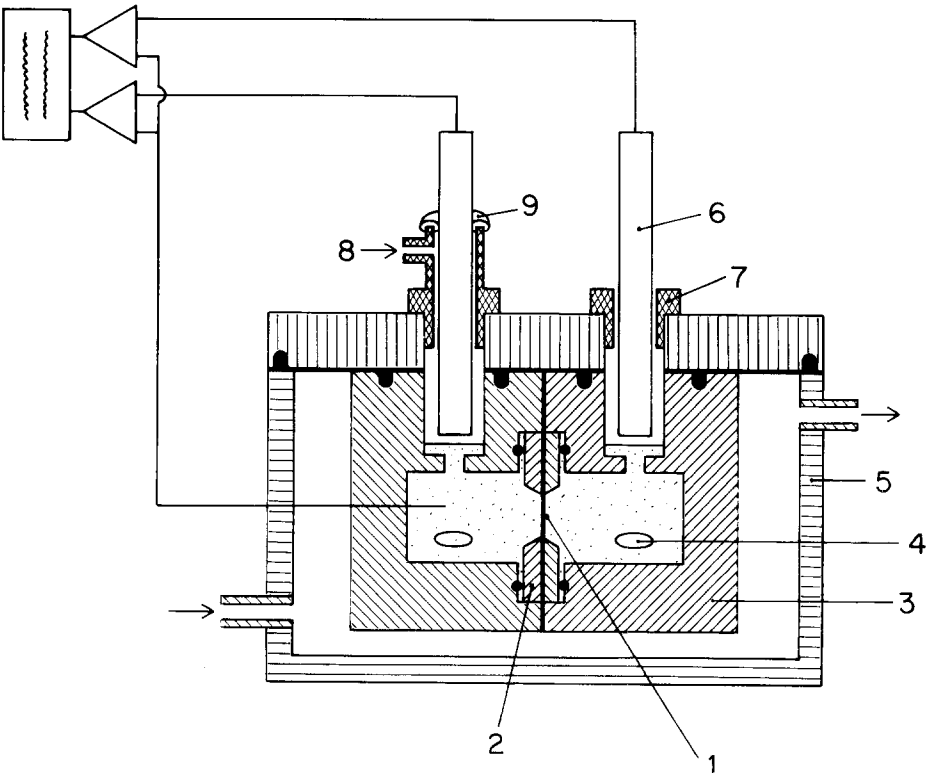

Fig. 1. Schematic representation of Lucite chamber and capacitance probes used for volume flow measurement across gallbladder epithelium. (*1*) gallbladder, (*2*) Lucite frame to hold the gallbladder, (*3*) Lucite chamber, (*4*) magnetic stirrer, (*5*) thermostated water mantle, (*6*) capacitance probe, (*7*) guide tubes, (*8*) pressure inlets, and (*9*) silicone rubber seals during pressure application. The capacitance probes can be readjusted above the waterface independently to any desired position (Wiedner, 1976)

in the half chambers, silicon rubber seals are applied around the probes and the guide tubes (*see* Fig. 1). The pressure can be increased on both sides of the gallbladder via pressure inlets in the guide tubes independently. The pressure is measured with differential metal manometers (Wallace & Tiernan, GMBH, Model 62-075 series 1500) and regulated with manostats (Aneroid Manostaten, FA-149, Wallace & Tiernan, GMBH). The chamber is thermostated at 20 ± 0.01 °C.

Permeability Measurements

The effect of stretching the tissue and the effect of osmotic or hydrostatic pressure on the permeability properties of the epithelium has been tested as follows: gallbladders are mounted as flat sheets between two Lucite half chambers as described by Van Os, Michels and Slegers (1976) (exposed area, 0.78 cm^2). The electrical potential difference across the gallbladder is measured via calomel half cells connected to the chamber solutions via Ringer/agar bridges. Current is passed through the tissue via Ag/AgCl electrodes. The electrical properties are checked by measuring the magnitude of the 2:1 NaCl dilution potential (75 mM NaCl replaced by sucrose in the mucosal solution) (Barry & Diamond, 1970). The permeability of the gallbladder to several nonelectrolytes has been determined by adding the solute in a ^{14}C- or ^{3}H-labeled form to one side and measuring the appearance on the other. Details have been published previously (Smulders & Wright, 1971).

Calculation of Permeability Constants

The hydraulic conductivity, L_p (cm/sec·atm) can be obtained from the linear law of irreversible thermodynamics:

$$J_v = -L_p \cdot (\Delta P - \sigma \Delta \pi) \tag{1}$$

where J_v(cm^3/sec·cm) is the volume flow in response to pressure gradients, ΔP(atm) and $\Delta \pi$(atm). σ is the reflection coefficient for the osmotic solute. For reasons of convenience L_p is converted to P_f (cm/sec), using the relation:

$$P_f = RTL_p / \bar{V}_w \tag{2}$$

where $\bar{V}_w$ is the partial molar volume of water. R and T have their usual meanings.

Results

Hydrostatic Pressure Gradients

Applying hydrostatic pressure gradients on the mucosal surface induces volume flows which can be monitored within seconds after raising the pressure. The volume flow is stable as long as the measurements are continued (up to 20 min). The flow force relation for mucosally applied pressures is shown in Fig. 2. This relation is linear for gradients up to 40 mbar. The slope yields a P_f value of 0.15 cm/sec. Above 40 mbar the slope tends to decrease, probably due to a decrease in the width

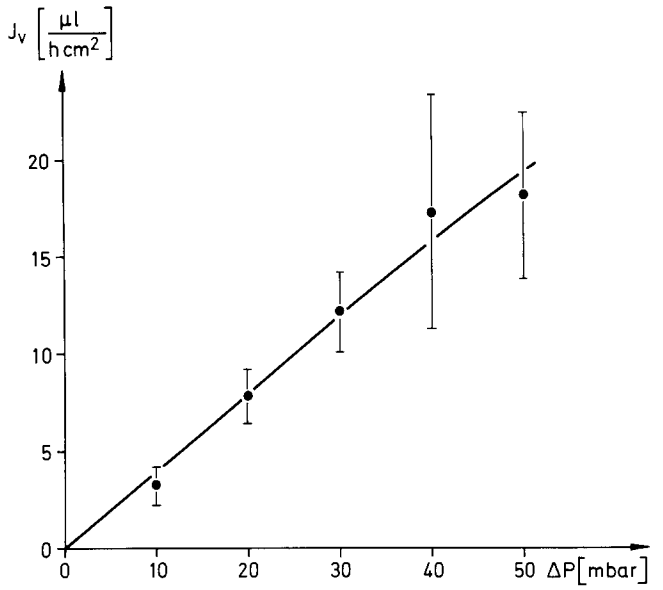

Fig. 2. Flow-force relation for volume flows induced by hydrostatic pressure gradients applied to the mucosal surface of gallbladder epithelium. The slope of the relation yields a P_f of 0.15 cm sec^{-1}. The points represent repeated measurements on 4 gallbladders. Each gradient is applied for 3 to 5 min

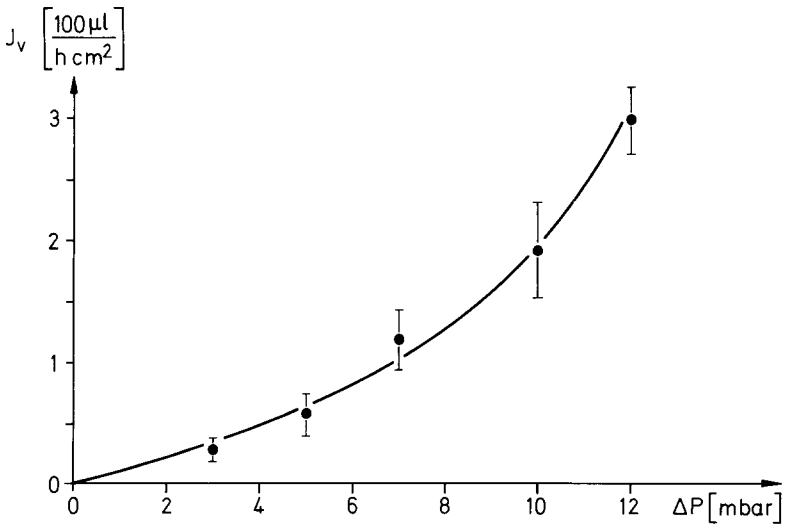

Fig. 3. Flow-force relation for volume flows induced by hydrostatic pressure gradients applied to the serosal surface of gallbladder epithelium. Between 0 and 5 mbar the P_f value is 4.5 cm sec^{-1}. The points represent measurements on 4 gallbladders

of the lateral intercellular spaces (Smulders, Tormey & Wright, 1972). In control experiments the influence of pressure on both sides simultaneously has been studied. The flow in response to a 30 mbar gradient does not change when the pressure on both sides is raised simultaneously by 50 mbar. In Fig. 3 the results are shown of experiments in which small pressure gradients are applied to the serosal surface. Also here the flow is constant within seconds after raising the pressure. Between 0 and 5 mbar the flow force relation is linear. With increasing pressures the relation deviates more and more from linearity. The P_f value between 0 and 5 mbar is 4.5 cm/sec, which is 30 times greater than for the reversed situation. Gradients larger than 10 mbar damage the epithelium irreversible since the flow rate due to 3 mbar is higher when the serosal side has been exposed to pressures above 10 mbar.

Osmotic Gradients

In everted gallbladders osmotic flow transients are observed when the mucosal solution is made hypertonic and when the flow is measured by weighing (Wright *et al.*, 1972). The following experiment is designed to find out whether osmotic flow transients are seen by the volumetric method. A small volume of 3 M sucrose is placed on the bottom of the mucosal half chamber. When the stirrer is switched on, a rapid mixing occurs between the mucosal fluid and the sucrose, hence an osmotic gradient is generated within seconds. In Fig. 4 such an experiment is shown. The abrupt decrease in the volume of the mucosal fluid is due to volume contraction caused by mixing concentrated sucrose with the Ringer's solution. (The same phenomenon is observed with parafilm as a membrane.) Within 5 sec after mixing, a volume flow is recorded from S to M. The flow rate is constant as long as the recording is continued (up to 20 min). No high initial flow rate is observed in contrast to the gravimetrical procedure. With the capacitance probes the volume of the bathing fluids is monitored and therefore the volume flow measured is a transmural flow. Shrinking or swelling of the tissue will not be detected, hence it is likely that the osmotic transients observed with a gravimetrical technique is related with a weight loss of the gallbladder tissue. For this reason the effect of osmotic gradients on the tissue wet wt has been studied. In Fig. 5 the results are shown. Within 5 to 10 min after applying osmotic gradients, a change in wet wt is observed. Mucosal hypertonicity reduces the wet wt by 22.5% ($n=13$), while serosal hyperto-

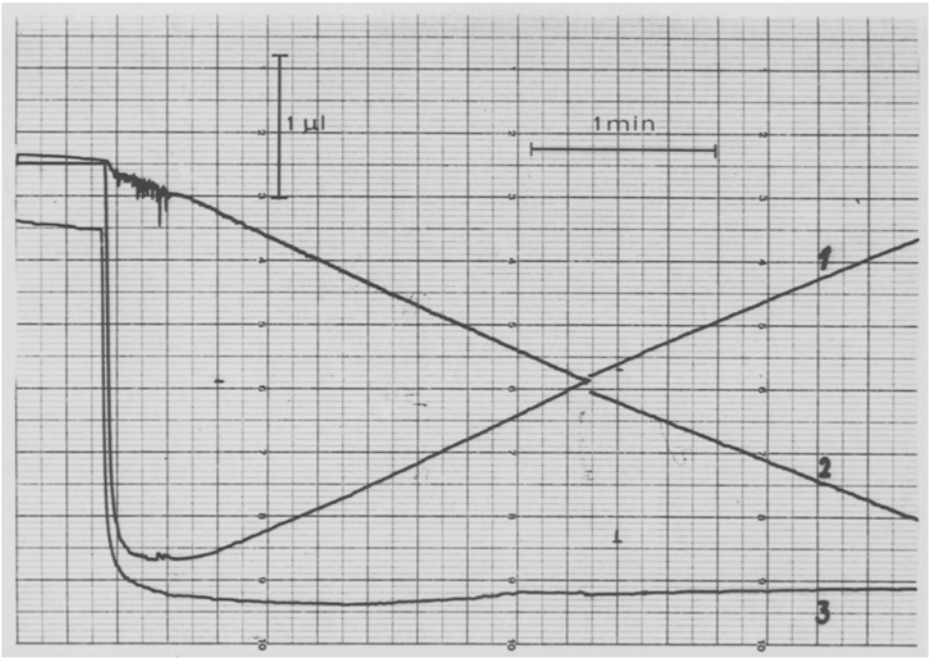

Fig. 4. Volumetric flow measurement by means of capacitance probes. At the beginning of the experiment the probe *1* above the mucosal compartment and probe *2* above the serosal compartment show no change of volume of either compartment. A few seconds after mixing (arrow) a water movement is recorded which is shown by a decrease (probe *2*) and increase (probe *1*) in volume of the serosal and mucosal solution, respectively. The third trace is the sum of probe signals *1* and *2*, indicating that there is no loss of water by evaporation or disappearance into the Lucite. In this experiment the mucosal solution had an osmolarity of 368 mosmol after mixing. The exposed bladder area in this experiment was 0.78 cm^2

nicity increases the wet wt by 31.0% ($n=6$). In some bladders, especially with larger gradients, the change in weight is irreversible. These observations are in agreement with the effects of osmotic gradients on the histology of gallbladders described by Smulders *et al.* (1972).

In Fig. 6 the flow-force relationship is shown for sucrose-induced volume flows from *S* to *M*. The relation is linear for concentrations up to 100 mM. With higher osmolarities the slope decreases as a result of collapse of the lateral intercellular spaces (Smulders *et al.*, 1972; Wright *et al.*, 1972). The P_f value in Fig. 6 is 9.3×10^{-3} cm/sec, which is about 2 to 3 times higher than values from gravimetrical measurements (Wright *et al.*, 1972). This difference is best explained by better stirring conditions in the chamber (Wiedner & Wright, 1975). Also, active trans-

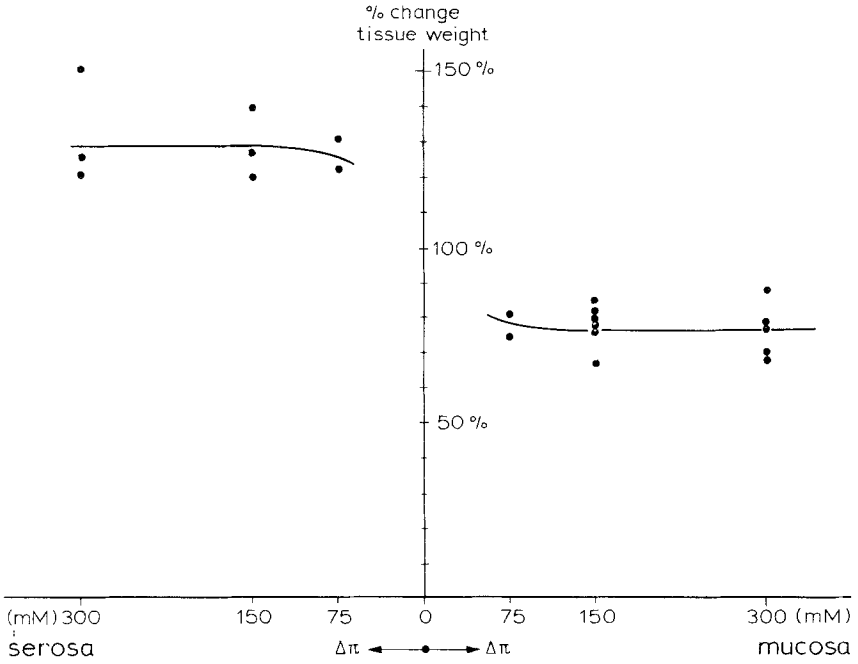

Fig. 5. Effect of osmotic gradients on wet wt of the gallbladder wall. Changes in wet wt have been expressed as percentage of the initial wet wt of the gallbladder incubated in normal Ringer's solutions. The horizontal axis gives the magnitude of the osmotic gradient. Gallbladder wet wt was determined as described under *Materials and Methods.* The control value of gallbladder wet wt was 83.6 ± 5.0 ($n=9$) mg/cm^2. The mean value after 5 min mucosal hypertonicity was 64.8 ± 5.2 ($n=13$) mg/cm^2, and after 5 min serosal hypertonicity 108.7 ± 6.5 ($n=6$)

port rates were twice as high in well-stirred chambers than in sac preparations (Van Os *et al.*, 1976). The osmotic P_f is about 15 times smaller than the hydrostatic P_f in Fig. 2.

Electrical Measurements

Osmotic flows are accompanied by so-called streaming potentials, due to salt polarization in unstirred layers (Wright *et al.*, 1972; Van Os *et al.*, 1976). Streaming potentials induced by additional sucrose in the mucosal solution are shown in Fig. 7*B*. Adding a few drops of concentrated sucrose to the well-stirred mucosal solution leads to a streaming potential which reaches a steady-state value within 5 sec, e.g., within the time course of the mixing process. Also, the transmural volume

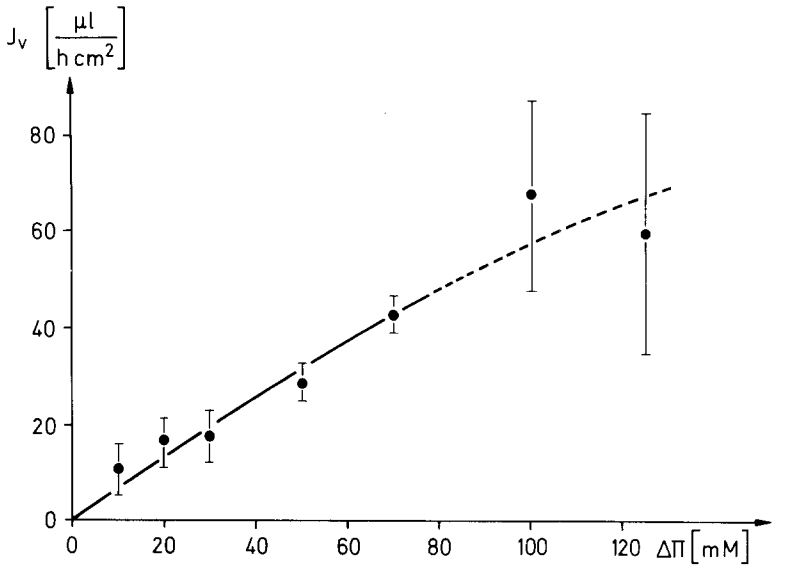

Fig. 6. Flow-force relation of osmotically induced volume flows across rabbit gallbladder epithelium. The mucosal solution is made hypertonic with respect to the serosal solution by the addition of sucrose. The flows were measured under steady-state conditions. The points represent repeated measurements on 4 gallbladders. The slope of the curve yields a P_f value of 9.3×10^{-3} cm sec^{-1}

flow in Fig. 4 has reached a steady-state value within 5 sec. The magnitude of the streaming potential is linearly related with the osmotic gradient up to 70 mosmol. Again this correlates well with the linear flow force relationship in Fig. 6. To measure streaming potentials induced by NaCl gradients, corrections have to be made for diffusion potentials due to the applied NaCl gradients. In Fig. 7*A* such a correction procedure is shown. This figure gives measured potentials across the gallbladder in the presence of additional NaCl in the mucosal solution. In one of the measurements sucrose is used to offset the osmolarity of the NaCl gradient, and in this situation there is no volume flow, hence no streaming potential. After correction for diffusion potentials, the magnitude of NaCl-induced streaming potentials is linearly related with the NaCl gradients up to 40 mM (Fig. 7*B*).

A 70-mM sucrose gradient induces a volume flow of 40 µl/hcm² and a streaming potential of 4 mV. Since a pressure gradient of 40 mbar on the mucosa and of 5 mbar on the serosa induces a flow of 15 and 60 µl/hcm², streaming potentials of 1.5 mV and of 6.0 mV can be anticipated. However, no streaming potentials can be observed during pressure filtration on either side (detection limit $\leqq 0.1$ mV). These observations

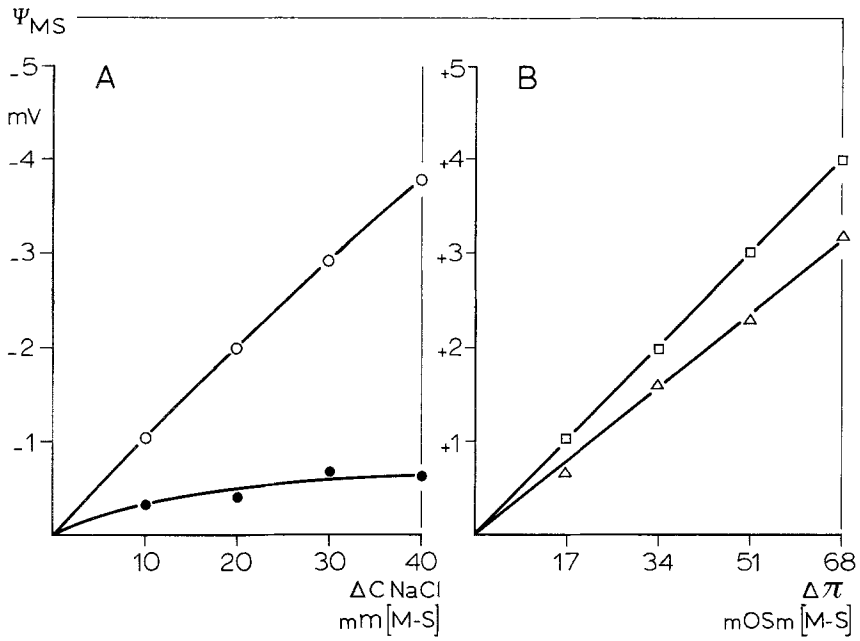

Fig. 7. Streaming potentials induced by NaCl and sucrose gradients in the mucosal fluid. (*A*): ○—○, Steady-state potentials due to additional NaCl in the mucosal solution in the absence of volume flows. The NaCl gradient is counterbalanced with sucrose in the serosal fluid. (e.g., 20 mM NaCl represents a gradient of 17 mosmol σ_{NaCl} is 0.7 to 0.8 with respect to sucrose (Van Os *et al.*, 1974; Monticelli, Celentano & Torelli, 1975), hence a 20 mM NaCl gradient is effectively balanced with 13 mM sucrose on the serosa). ●—●, Steady-state potentials due to additional NaCl in the mucosal solution in the presence of volume flows. (*B*): □—□, Streaming potentials due to additional sucrose in the mucosal fluid. △—△, Streaming potentials due to NaCl gradients. These values are calculated as the difference between the two lines in *A*

suggest that pressure-induced flows represent bulk flow with identical salt concentrations as in the bathing fluids. When this is the case no solute polarization can be expected. In addition, the magnitude of the 2:1 NaCl dilution potential (10 to 12 mV) is not influenced by pressures up to 50 mbar on the mucosa nor by pressures up to 10 mbar on the serosa. With serosal pressures of 5 and 10 mbar, the resistance of the gallbladder did not change. These control experiments indicate that pressure application within the range used in this study does not destroy the permselectivity of the shunt pathway.

Nonelectrolyte Permeabilities

Table 1 shows the effect of 50 mbar mucosal pressure on fluxes (*M* to *S*) of urea, ethylene glycol, and inulin. The small decrease in permeabil-

Table 1. Influence of hydrostatic pressure in the mucosal bathing fluid on nonelectrolyte permeability of gallbladder epithelium

$J_{M\to S}$	P in 10^{-6} cm/sec P_o	$\Delta P \simeq 50$ mbar (% of initial value)
^{14}C-urea	51.2±12.4	69± 5% (n=4)
^{14}C-ethylene glycol	17.9± 4.1	86±11% (n=4)
^{3}H-inulin	1.2± 0.2	92± 4% (n=8)

The permeability to nonelectrolytes during a pressure gradient of 50 mbar is expressed as a percentage of the control value immediately before pressure application. The flux of nonelectrolytes was measured in the direction mucosa to serosa. In this situation the volume flow from M to S averaged 18 µl/hcm^2.

ity may be related to changes in the lateral intercellular spaces. However, the decrease in inulin permeability is smaller than the change in urea permeability. These results show that gallbladder epithelium withstands mucosal pressure easily.

Table 2 shows that pressure applied to the serosal surface causes an enormous increase in S to M fluxes. Commercially available ^{3}H-methoxyinulin, used in these experiments, may contain a small amount of low mol wt substances (Munck & Rasmussen, 1977). For this reason we have included flux studies with the more homogeneous ^{14}C-polyethylene glycol, but the results obtained with inulin and PEG are essen-

Table 2. Influence of a hydrostatic pressure on the serosal surface on nonelectrolyte permeability of gallbladder epithelium

	Permeabilities P in 10^{-6} cm/sec		
	Control	ΔP=5 mbar	ΔP=10 mbar
$J_{S\to M}$:			
^{14}C-ethylene glycol	15.4±2.5	26.9±7.5	77.8±16.3 (n=6)
^{3}H-inulin	1.2±0.2	10.1±6.5	48.2±10.0 (n=10)
^{14}C-poly ethylene glycol	0.4±0.1	3.1±1.8	36.4± 8.6 (n=4)
$J_{M\to S}$:			
^{14}C-ethylene glycol	18.0±2.6	14.7±3.2	11.8± 3.6 (n=4)
^{3}H-inulin	1.7±0.3	1.1±0.2	0.7± 0.2 (n=4)

The volume flows with 5 and 10 mbar were 60 and 180 µl/hcm^2, respectively. Fluxes were measured during periods of 45 min. In 40% of the bladders the permeability to inulin had increased with a factor of 1.5 after 10 mbar serosal pressure application. In the others no change in permeability was observed after pressure application.

Table 3. Inulin permeability during osmotic volume flows and during active reabsorption in rabbit gallbladder

		Inulin permeability in 10^{-6} cm/sec	
A.	Osmotic flow $M \rightarrow S$	$\Delta\Pi = 0$	$\Delta\Pi = 300$ mM sucrose
	P_{inulin} $(M \rightarrow S)$	1.7 ± 0.6	1.6 ± 0.6 $(n=3)$
	P_{inulin} $(S \rightarrow M)$	1.6 ± 0.7	3.2 ± 0.8 $(n=3)$
B.	Active reabsorption	37 °C	37 °C + ouabain
	P_{inulin} $(M \rightarrow S)$	2.4 ± 0.4	1.8 ± 0.3 $(n=5)$
	P_{inulin} $(S \rightarrow M)$	3.1 ± 0.5	1.8 ± 0.4 $(n=5)$

The volume flows in the presence of a 300 mM sucrose gradient and during active reabsorption are between 60 and 100 µl/hcm^2 (Wright *et al.*, 1972; Van Os *et al.*, 1976). Inulin fluxes were measured during 1 hr periods. In condition *B* the bladder was bathed with 5×10^{-4} M oubain for 1 hr before the control flux of inulin was determined in order to inhibit the active transport in rabbit gallbladder (*see* Van Os & Slegers, 1971).

tially similar. Table 2 also shows that, concomitantly, there is a significant, but substantially smaller, decrease in the *M* to *S* fluxes.

Table 3 summarizes the effects of osmotic flows and solute-linked fluid transport on inulin fluxes. In both conditions, despite the net water flow of 60 to 100 µl/hcm^2 from *M* to *S*, there is a small but significant increase in the inulin fluxes from *S* to *M*. On the other hand, there is no significant effect on inulin fluxes from *M* to *S*. Munck and Rasmussen (1977) described a similar phenomenon during fluid absorption in rat jejunum in vitro. These results are in contrast to those observed with serosal pressures, Table 2, where water flows from *S* to *M* of 60–180 µl/hcm^2 produced an increase in *S* to *M* fluxes and a decrease in *M* to *S* fluxes of nonelectrolytes.

Discussion

In this study P_f values of gallbladder epithelium have been measured using a continuous volumetric method based on capacitance measurements. The time resolution of volume-flow measurements is on the order of seconds, which is an improvement of two orders of magnitude over gravimetrical measurements. Small osmotic and hydrostatic pressure gradients have been used and, in the range where the flow-force relation is linear, the linear laws of irreversible thermodynamics have been applied. The P_f values are: 9.3×10^{-3} cm/sec for sucrose gradients

($J_v^{S\to M}$), 0.15 cm/sec for mucosal pressure gradients, and 4.5 cm/sec for serosal pressure (between 0 and 5 mbar).

Osmosis

The osmotic P_f value is the highest steady-state value reported for rabbit gallbladder so far. Although this value is for S to M flows, a similar value can be expected for M to S flows, since gallbladder epithelium behaves symmetrically towards small osmotic gradients (Wright *et al.*, 1972; Van Os *et al.*, 1976). Osmotic flows are accompanied by solute polarization in the unstirred layers and, therefore, the effective osmotic gradient will be smaller than the applied ones.

It has been proven that streaming potentials reflect solely these polarization effects (Wedner & Diamond, 1969; Van Os *et al.*, 1976). With help of the data in Fig. 7 it is possible to estimate the extent to which the applied osmotic gradient is reduced. Figure 7*B* shows that an osmotic flow in response to 50 mosmol sucrose induces a streaming potential of about 3 mV. In Fig. 7*A*, 3 mV corresponds with a diffusion potential measured between 180 and 150 mM NaCl solutions on either side of the epithelium. Since 30 mM NaCl constitutes an osmotic force of 40 mosmol ($\sigma_{NaCl} \simeq 0.8$, the osmotic coefficient $\simeq 0.85$), the applied 50 mosmol gradient is effectively reduced to 10 mosmol. Hence, the osmotic P_f, after correction for polarization effects, has a value of approximately 0.05 cm/sec. It has to be emphasized that corrections for polarization effects based on streaming potentials are only related to polarization effects seen by the permselective shunt pathway and that polarization effects across the cell membranes are not taken into account.

With the volumetric method, osmotic flow transients and high initial flow rates are not observed which are in contrast to gravimetrical measurements. This difference is simply explained by the fact that transmural flows are recorded with the volumetric method. Changes in the water content of the tissue will be detected by weighing but not by monitoring the volume of the bathing solutions. Wright *et al.* (1972) explained the osmotic flow transients by solute polarization. However, this explanation is unlikely in view of the time courses of both processes, e.g., the flow transients have a time course of about 15 min whereas the streaming potentials have reached a steady state within 5 sec. The changes in wet wt of gallbladders during osmosis given in Fig. 4 have time courses which correlate very well with the flow transients. Swelling and shrinking

of the bladder is most likely an in vitro artefact, since water has to cross additional barriers, the serosal muscle and collagen layers, in contrast to the in vivo situation. These additional layers constitute significant barriers to bulk flow (Smulders *et al.*, 1972). The question is now whether these osmotic flow transients, related to swelling and shrinking, provide information about the P_f of the epithelium. The answer to this question remains obscure since it is unknown from where the water comes. In the case of mucosal hypertonicity, the osmotic transients can be due to shrinking of the cells and/or water out of the submucosal space via the cells or via the junctional route. Therefore, estimates of the "true" osmotic P_f based on extrapolations of osmotic flow transients may not be very realistic.

One of the aims of this study was to improve the time resolution of volume flow measurements across epithelial membranes. One could argue that a time resolution on the order of seconds may not be good enough and that methods are needed with a time resolution smaller than 1 sec in order to study flow transients and polarization effects. However, even in the best stirring condition, the unstirred layer thickness on the mucosal side is about 50 μm (Bindslev, Tormey & Wright, 1974; Wiedner & Wright, 1975). The half time for diffusion of sucrose across 50 μm is already greater than 1 sec, and therefore a time resolution smaller than 1 sec will not be of much help.

In view of the above discussion it seems not very useful to pay much attention to the question what the "true" osmotic P_f value may be. Polarization effects may also occur during solute-linked water transport in vivo. Due to the pump activity in the baso-lateral membranes, polarization effects across that membrane will be minimal, but polarization may occur across the mucosal membrane. The corrected osmotic P_f value from this study (0.05 cm/sec) seems a reasonable estimate of the "effective" P_f, operating during solute-linked water transport. The "true" value will not be much greater than 0.05 cm/sec, since the hydrostatic equivalent is 0.15 cm/sec. It is very likely that in the latter situation most of these flows are generated across pathways where the reflection coefficients for NaCl and sucrose are significantly less than unity. Reasons in favor of this view will be discussed below.

Hydrostatic Pressure

First of all, it should be mentioned that small serosal pressure generates enormous volume flows in proximal tubules, small intestine and gallblad-

der alike. In our study serosal pressure of 5 mbar yields a hydrostatic P_f value of 4.5 cm/sec, comparable to 8.8 cm/sec in rat proximal tubules (Sato, 1975) and 2.9 cm/sec in dog small intestine (Hakim & Lifson, 1969); both values have been obtained with 4 mbar gradients.

At least we have shown that these small pressures do not destroy the permselectivity of the shunt pathway nor do they reduce the tissue resistance substantially. This is in agreement with histological studies of Tormey and Diamond (1967), who described that serosal pressure up to 5 mbar did not rupture the epithelium. In addition, we have shown that serosal pressure of 5 to 10 mbar, but neither osmotic nor solute linked flows, exert a solvent drag effect on inulin and PEG 4000 fluxes. This observation makes it highly unlikely that serosal pressure gradients generate flows across the cellular route.

The question arises whether these large volume flows are generated across the junctional route or whether they are generated across newly formed pores in the epithelial mosaic. One possibility is to think of bulk flow via the junctional route, where the junctions have to be thought of as narrow continuous slits around the cells. The slit width necessary to accomodate the volume flow can be calculated from the relation:

$$B^3 = \frac{3\eta 1 V}{2NW\Delta P} \tag{3}$$

(Bird, Steward & Lightfoot, 1960) where B is the half distance between opposing junctional membranes, $\eta = 0.01$ poise, $1 = 2 \times 10^{-5}$ cm (length of junctional route, Tormey and Diamond (1967)), $V = 16.7 \times 10^{-6}$ cm^3/cm^{2}sec (average flow velocity due to 5 mbar, Fig. 3; the actual flow velocity in these spaces may be much higher), $N = 6 \times 10^6$ cells/cm^2 (cells arranged as hexagonals; Van Os, de Jong & Slegers, 1974), $W = 7.5 \times 10^{-4}$ cm (half the cell circumference), $\Delta P = 4.9 \times 10^3$ dyne/cm^2 (5 mbar). The slit width has to be > 60 Å in order to accomodate the flow. This would imply an inulin permeability $> 10^{-4}$ cm/sec and a resistance $< 1 \Omega$cm^2. These values are two orders of magnitude out of range with the observed ones, which suggests that it is unlikely that water is filtered through slits homogeneously around the cells. Assuming circular pores instead of continuous slits, similar calculations lead to the results tabulated in Table 4. This table also includes calculations for mucosal pressure induced flows.

The number $N = 10^7$ pores/cm^2 has been postulated previously to explain the sucrose permeability of rabbit gallbladder (Wright *et al.*,

Table 4. Hypothetical pore radii and number of pores per cm^2 to accomodate volume flows due to pressure gradients

Pores/cm^2 (N)	Serosal pressure of 5 mbar ($J_V = 60$ µl/hcm^2)			Mucosal pressure of 40 mbar ($J_V = 15$ µl/hcm^2)		
	r (10^{-8} cm)	P_{inulin} (10^{-6} cm/sec)	R (Ωcm^2)	r (10^{-8} cm)	P_{inulin} (10^{-6} cm/sec)	R (Ωcm^2)
10^7	363	31	4.8	155	5.6	26
10^5	1150	3.1	48	495	0.6	260
10^3	3630	0.3	480	1550	0.06	2600

In the table are summarized results of calculations of hypothetical pore radii which are needed to accomodate the volume flows induced by pressure gradients. The number of pores per cm^2 are set at 10^7, 10^5 or 10^3. The radii are obtained by using the equation:

$$V = N \frac{\Pi r^4 \Delta P}{8 \eta l} \tag{4}$$

(Poiseuille's law) where symbols and values are the same as given for Eq. (3). With the obtained pore radii, the inulin permeability and the electrical resistance were calculated as follows:

$$P_{inulin} = \frac{N \Pi r^2 D}{l} \tag{5}$$

where $D = 1.5 \times 10^{-6}$ cm^2/sec (diffusivity for inulin, Van Os *et al.*, 1974).

$$R = \frac{\rho l}{N \Pi r^2} \tag{6}$$

where $\rho = 100$ Ω/cm, the specific resistance of Ringer's solution at 20 °C (Robinson Stokes, 1970).

1972; Van Os *et al.*, 1974). Although the calculations in Table 4 are nothing more than rough estimates, the tendency is quite clear. Only a relatively few large pores are compatible with the large volume flows and the observation that the resistance is unchanged by small serosal pressures. Therefore it is reasonable to assume that the mechanism of serosal pressure-induced secretion consists mainly in rupturing of zonulae occludentes between a small number of cells. According to Tormey and Diamond (1967) pressure of 5 mbar does not lead to ruptured junctions. However, the large flows can be accounted for when less than $0.1\,^0/_{00}$ of the junctional structures between three joining cells dilate or rupture to form pores of about 0.5 µm wide. It is likely that such a small number of pores are not detectable in histological studies.

Junctions between three cells may be most sensitive to serosal pressure, for in a recent study by Spring and Hope (1978) on living gallbladders, it was shown that in the presence of serosal pressure, "lakes" of fluid were frequently seen below these particular junctions. In support of our interpretation is the absence of any measurable streaming potential during serosal and mucosal pressure gradients. It is obvious that bulk flow through pores of this size will have an identical ionic composition as the bathing fluid, and therefore no solute polarization can be expected. These large pores will not contribute substantially to osmotic flows since the sucrose or NaCl reflection coefficients in these pores will be near zero. Therefore, osmotic and hydrostatic P_f values cannot be compared; they simply represent different pathways through the epithelium. Moreover, our interpretation offers also an explanation for the enhanced blood to lumen flux of inulin in rabbit small intestine (Humphreys & Early, 1971) and in *Necturus* proximal tubule (Boulpaep, 1972) during plasma volume expansion.

Whether ruptured junctions reseal after pressure application cannot be concluded from our inulin flux measurements, since a small number of pores will not lead to a significant increase in the inulin permeability. However, the slight increase in P_{inulin} in some of the bladders after 10 cm H_2O and the fact that pressures greater than 10 cm H_2O markedly increased the flow due to 3 cm H_2O suggest that serosal pressure of 10 cm H_2O and greater produces irreversible ruptures.

Route of Water Flow During Osmosis and Active Solute Transport

The enhanced S to M inulin fluxes observed during osmosis and net solute-linked water transport (Table 3) suggest that in both situations the net M to S water flow is accompanied by a significant paracellular backflux of water into the lumen. The S to M water flow is probably the result of a small serosal pressure caused by the hydraulic barrier of the muscle layer. These observations can be taken as a hint that net solute-linked water transport results from transcellular instead of paracellular water movement. Moreno (1975) postulated two separate paracellular pathways in gallbladder epithelium, one leakage pathway for sucrose, inulin, and Cl^-, and in addition to that a cation selective pathway. The calculated "best-fit pore radius" for the cation channel was 4.5 Å in rabbit gallbladder, for inorganic as well as organic cations (Moreno & Diamond, 1975). One could postulate that during active sol-

ute transport, salt gradients across the junctional cation channels drag water directly into the lateral intercellular spaces. Using flow equation (3) it can be calculated that in order to accomodate a flow rate of 100 $\mu l/hcm^2$ (normal active transport rate) through continuous slits with a half slit width of 4.5 Å, a pressure gradient of 10^7 dynes/cm^2 is needed, which is equivalent to 420 mosmol or to a salt gradient of about 250 meq assuming a reflection coefficient of unity. It is highly unlikely to expect such a hypertonicity in the spaces. Gupta, Hall and Naftalin (1978) estimated a hypertonicity between 10 and 40 meq in the lateral intercellular spaces of rabbit ileum, while Machen and Diamond (1969) arrived at an estimate of 10 meq in rabbit gallbladder. Therefore, it seems that the junctional waterflow during active solute transport is less than 10% of the net water flow. On the other hand, if most of the water flow is through the cation shunt pathway a solvent drag effect on unidirectional Na fluxes has to be anticipated. We know of two studies in which Na fluxes from *M* to *S* and from *S* to *M* have been measured in the presence and absence of solute-coupled water transport. Taylor, Wright, Schultz and Curran (1968) report a decrease in Na fluxes in both directions after inhibition of fluid transport in rabbit small intestine; and Andreoli, Schafer and Patlak (1978) report that the Na flux from blood to lumen in rabbit proximal tubules is independent of volume absorption. These observations support the view that the cation shunt pathway is not the major route for water during solute-linked water transport. However, to conclude, the role of the paracellular pathway in isotonic transport can be evaluated only when the hydraulic conductivity of this route has been measured. How this can be done is not yet clear.

This study was in part supported by Public Health Service Grant NS 09666. We are indebted to Professor R. Schlögl for his encouragements. Mr. M.D. de Jong is gratefully acknowledged for excellent technical assistance.

References

Andreoli, T.E., Schafer, J.A., Patlak, C.F. 1978. Mechanisms for salt and water transport in the mammalian proximal straight tubule. *In:* Membrane Transport Processes. J.F. Hoffman, editor. Vol. I, pp. 385–431. Raven Press, New York

Barry, P.H., Diamond, J.M., 1970. Junction potentials, electrode standard potentials, and other problems in interpreting electrical properties of membranes. *J. Membrane Biol.* **3**:93

Bindslev, N., Tormey, J.McD, Wright, E.M. 1974. The effects of electrical and osmotic gradients on lateral intercellular spaces and membrane conductance in a low resistance epithelium. *J. Membrane Biol.* **19**:357

Bird, R.B., Steward, W.E., Lightfoot, E.N. 1960. Transport Phenomena. Chapter 2, p. 34. John Wiley and Sons, New York

Boulpaep, E. 1972. Permeability changes of the proximal tubule of *Necturus* during saline loading. *Am. J. Physiol.* **222**:517

Gupta, B.L., Hall, T.A., Naftalin, R.J. 1978. Microprobe measurement of Na, K and Cl concentration profiles in epithelial cells and intercellular spaces of rabbit ileum. *Nature (London)* **272**:70

Hakim, A.S., Lifson, N. 1969. Effects of pressure on water and solute transport by dog intestinal mucosa in vitro. *Am. J. Physiol.* **216**:276

House, C.R. 1974. Water transport in cells and tissues. Edward Arnold, London

Humphreys, M.H., Earley, L.E. 1971. The mechanism of decreased intestinal sodium and water absorption after acute volume expansion in the rat. *J. Clin. Invest.* **50**:2355

Lerche, D. 1976. Temporal and local concentration changes in diffusion layers at cellulose membranes due to concentration differences between the solutions on both sides of the membrane. *J. Membrane Biol.* **27**:193

Machen, T.E., Diamond, J.M. 1969. An estimate of the salt concentration in the lateral intercellular spaces of rabbit gall-bladder during maximal fluid transport. *J. Membrane Biol.* **1**:194

Monticelli, G., Celentano, F., Torelli, G. 1975. Sodium chloride reflection coefficient in rabbit gallbladder. *Biochim. Biophys. Acta* **401**:41

Moreno, J.H. 1975. Routes of non-electrolyte permeability in gallbladder. Effects of 2,4,6-triaminopyrimidinum (TAP). *J. Gen. Physiol.* **66**:117

Moreno, J.H., Diamond, J.M. 1975. Cation permeation mechanisms and cation selectivity in "tight junctions" of gallbladder epithelium. *In:* Membranes—A Series of Advances. G. Eisenman, editor. Vol. 3, p. 383. Marcel Dekker, New York

Munck, B.G., Rasmussen, S.N. 1977. Paracellular permeability of extracellular space markers across rat jejunum in vitro. Indication of a transepithelial fluid circuit. *J. Physiol. (London)* **271**:473

Robinson, R.A., Stokes, R.H. 1970. Electrolyte solutions, p. 466. Butterworths, London

Sato, K. 1975. Reevaluation of micropuncture techniques: Some of the factors which affect the rate of fluid absorption by the proximal tubule. *In:* Current Problems in Clinical Biochemistry: 4. Biochemical Aspects of Renal Function, p. 175–187. S. Angielski and U.C. Dubach, Editors H. Huber, Bern-Stuttgart-Vienna

Smulders, A.P., Tormey, J.McD, Wright, E.M. 1972. The effect of osmotically induced water flows on the permeability and ultrastructure of the rabbit gallbladder. *J. Membrane Biol.* **7**:164

Smulders, A.P., Wright, E.M. 1971. The magnitude of nonelectrolyte selectivity in the gallbladder epithelium. *J. Membrane Biol.* **5**:297

Spring, K.R., Hope, A. 1978. Size and shape of the lateral intercellular spaces in a living epithelium. *Science* **200**:54

Taylor, A., Wright, E.E., Schultz, S.G., Curran, P.F. 1968. Effects of sugars on ion fluxes in intestine. *Am. J. Physiol.* **214**:836

Tormey, J.McD, Diamond, J.M. 1967. The ultrastructural route of fluid transport in rabbit gallbladder. *J. Gen. Physiol.* **50**:2031

Van Os, C.H., Slegers, J.F.G. 1971. Correlation between (Na-K) activated ATPase activities and the rate of isotonic fluid transport of gallbladder epithelium. *Biochim. Biophys. Acta* **241**:89

Van Os, C.H., Jong, M.D. de, Slegers, J.F.G. 1974. Dimensions of polar pathways through rabbit gallbladder epithelium. The effect of phloretin on nonelectrolyse permeability. *J. Membrane Biol.* **15**:363

Van Os, C.H., Michels, J.A., Slegers, J.F.G. 1976. Effects of electrical gradients on volume flows across gallbladder epithelium. *Biochim. Biophys. Acta* **443**:545

Wedner, H.J., Diamond, J.M. 1969. Contributions of unstirred-layer effects to apparent electrokinetic phenomena in the gallbladder. *J. Membrane Biol.* **1**:92

Wiedner, G. 1976. Method to detect volume flows in the nanoliter range. *Rev. Sci. Instrum.* **47**:775

Wiedner, G., Wright, E.M. 1975. The role of the lateral intercellular spaces in the control of ion permeation across the rabbit gallbladder. *Pfluegers Arch.* **358**:27

Wright, E.M., Smulders, A.P., Tormey, J.McD. 1972. The role of the lateral intercellular spaces and solute polarization effects in the passive flow of water across the rabbit gallbladder. *J. Membrane Biol.* **7**:198